www.czasopisma.pan.pl PAN www.journals.pan.pl

ARCHIVES of FOUNDRY ENGINEERING

ISSN (2299-2944)
Volume 2023
Issue 1/2023

11 – 16

10.24425/afe.2023.144274

2/1

Published quarterly as the organ of the Foundry Commission of the Polish Academy of Sciences

Investment Casting of AZ91 Magnesium Open-Cell Foams

H. Kapłon, A. Dmitruk, K. Naplocha *
Wroclaw University of Science and Technology, Poland
* Corresponding author: Email address: krzysztof.naplocha@pwr.edu.pl

Received 31.08.2022; accepted in revised form 07.11.2022; available online 31.01.2023

Abstract

The process of investment casting of AZ91 magnesium alloy open-cell porosity foams was analysed. A basic investment casting technique was modified to enable the manufacturing of magnesium foams of chosen porosities in a safe and effective way. Various casting parameters (mould temperature, metal pouring temperature, pressure during metal pouring and solidifying) were calculated and analysed to assure complete mould filling and to minimize surface reactions with mould material. The foams manufactured with this method have been tested for their mechanical strength and collapsing behaviour. The AZ91 foams acquired in this research turned out to have very high open porosity level (>80%) and performed with Young's modulus of ~30 MPa on average. Their collapsing mechanism has turned out to be mostly brittle. Magnesium alloy foams of such morphology may find their application in fields requiring lightweight materials of high strength to density ratio or of high energy absorption properties, as well as in biomedical implants due to magnesium's high biocompatibility and its mechanical properties similar to bone tissue.

Keywords: Innovative foundry technologies and materials, Metal foams, Investment casting, Magnesium alloy

1. Introduction

Porous materials are a special material class that offers unique properties and various possible applications. Many natural materials that may be included in this category, such as sponges, coral, zeolites, wood or cork, have been used for centuries thanks to their structure, low density and good absorption properties. Materials engineering and taking inspiration from nature allowed to create man-made porous materials that can be mastered and fit to very specific requirements. Metal foams are a very specific category of cellular materials. Unlike polymeric foams, they can withstand elevated temperatures and UV light and they're less brittle than ceramic foams [1]. Because of their particularly high strength-to-weight and stiffness-to-weight ratios, they are used in the automotive, aircraft and spacecraft industries to lower the vehicles' mass and fuel consumption [2-3], as well as in lightweight construction materials. Metallic foams highly developed specific surface area is a valuable feature in the production of noise-cancelling materials [4], heat exchangers [5-6], filters [7], condensers in reactors [8-9] and catalytic beds in the chemical industry [10-11]. Their good performance in energy absorption is useful as wave absorbing material, for example, as explosion protectors [12], vibration absorbers [13] and bumpers [14]. Foams with certain cell structures are also a promising material for bone implants construction since they resemble the cancellous bone tissue and provide a good scaffold for growing cells [15].

Metal foams, especially aluminum ones, have been widely researched in the last few decades. However, magnesium foams are a far less explored field that increased in popularity in recent years. Magnesium is the lightest of all metals that can be used for construction purposes which makes it an interesting material for producing metal foams. Their high strength-density ratio, high specific energy absorption and good impact resistance are highly desirable features [16]. Additionally, magnesium's high biocompatibility [17] and mechanical properties close to those of bone tissue [18] make it a promising candidate for future implantology techniques.

One of the most popular techniques for the production of open-pore metallic foams is by infiltration methods and most commonly by a space-holder method [19-20], but this method has numerous difficulties that are solved by the investment casting method that was modified by the authors to enable a safe and precise process of magnesium foams casting. Magnesium casting is a particularly dangerous process due to its combustion in the air when heated to its liquidus temperature [21]. Another problem in Mg foam casting is that the salt pattern method produces foams with an often uneven pore distribution and with not fully open pore structure that makes the salt pattern difficult to be washed out. The authors managed to overcome those difficulties and hazards by using the polyurethane (PUR) foam pattern method with investment casting in a protective atmosphere. In this study, a technology for production of open-pore AZ91 Mg alloy foam by means of investment casting is described and optimized to manufacture foams of varying porosities and pore sizes. The casting parameters and foams surface morphology and compressive behaviours are analysed.

2. Materials and methods

The magnesium foams were produced from AZ91 alloy (9 wt.% of Al, 0.13 wt.% of Mn, and 0.7 wt.% of Zn), widely used in permanent and pressure casting due to the good cast-ability, relatively high mechanical properties, fine microstructure and high-quality external surface. Alloy comprises α-Mg phase with numerous intermetallic compounds of $\beta\text{-}Mg_{17}Al_{12}$ phase distributed along its grans. The presence of aluminum contributes to developing the oxide layer and improves corrosion resistance as well as mechanical properties [22].

The manufacturing of foam blocks was based on the evaporation of PUR foam pattern in the investment casting technology. The steps of the process are illustrated in Figure 1.

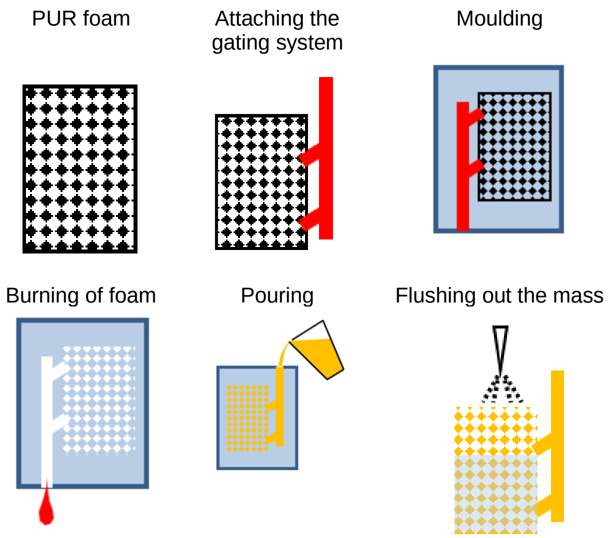

Fig. 1. Scheme of the investment casting of AZ91foam

For creating a mould cavity, polyurethane foams characterised by specific mesh size were selected. Described by pores per inch parameter (PPI), two kinds of foams were produced: 10 PPI with an average 6 mm pore size and 20 PPI with approximately 3 mm pore size. The open porosity feature can be controlled by coating the polyurethane structure with a wax-based slurry. Exemplary magnesium foam structure is presented in Fig. 2. The moulds were made in Ø130 mm casting flasks, using Ransom & Randolph Argentum gypsum-based investment. After hardening and drying mould with PUR foam was subjected to heat treatment, during which the polyurethane was burnt away living cavity as an exact copy of the pattern. The heat treatment comprises the following processes:

- dehydrating at 150°C and dewaxing at 370°C,
- burning and firing organic material at 700°C for 2 hours,
- cooling down to a pouring temperature of 500-650°C.

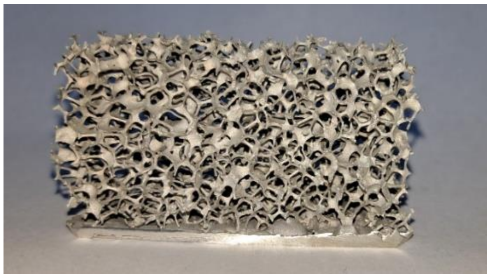

Fig. 2. AZ91 magnesium alloy sample (55x35x20 mm) produced from 20 PPI polyurethane foam

The foams were cut into cuboid samples of a cross-section ~8 cm^2 and 4 cm in height. Their porosity was measured by Archimedes's principle and its value varied between 80 and 90%. The samples were tested for their compressive behaviour using the universal testing machine Tinius Olsen H25KT with the test speed set as 10 mm/min, with a maximum 10 kN load. The crushed and uncrushed foams were analysed using SEM microscope Hitachi TM-3000 with EDS detector to examine their microstructure, surface composition and collapsing mechanism.

3. Results and discussion

3.1. Casting parameters analysis

The prepared portion of the AZ91 magnesium alloy was melted in steel crucible and poured in an experimental temperature range: 660–760°C, under SF6 protective gas atmosphere. The proper mould and pouring temperatures were adjusted according to the calculations and experimental trials. The process conditions and parameters depending on multiple factors, such as the shape and size of the gating system, the vacuum level, and the flask dimension and mould mass, should be strictly controlled. The most important casting parameters ensuring effective infiltration of the intricate mould cavity and simultaneously hindering the adverse reaction between the metal and the ceramic material are: the temperature of the mould and the liquid metal, as well as the value of vacuum creating pressure acting on metal in the cavity. The process parameters can be classified into groups related to (1) the properties of the casting mould, (2) the melting and pouring conditions and (3) the quality of the liquid alloy. During the pouring of the mould stream of liquid metal penetrates through very small and narrow channels. See Fig. 3 showing spatial structure formed by thin struts. Depending on the ceramic wall temperature it may cool quickly, crystallize and form solid skin. Very important is the thermal diffusivity of the mass. Considering low thermal conductivity and medium specific heat of investment moulding materials, it can be expected that at rapid pouring and filing, molten metal preheats a relatively thin layer of the mould surface. Therefore, conditions for possibly fast filling i.e. high-pressure gradient created by vacuum in the autoclave, must be provided. Temperature of the flowing liquid stream is maintained and metal can attain deep channels in the mould. Under vacuum atmospheric external pressure, calculated with formula (1):

$$P = P_{mould} + \frac{\gamma}{R} \tag{1}$$

should overcome the resistance of the mould - P_{mould}, produced by the existing gases inside the cavity and expansion of a new metal–mould interface. Additionally, the meniscus-shaped metal front of radius R will be restricted by the surface tension γ.

Figure 3a shows the structure of the foam exhibiting high porosity of 92% manufactured on the basis of the original 10 PPI PUR foam size. Surface of the single strut (Fig. 3b) is slightly affected by ceramic material, which can react with molten metal. It is necessary to determine the possibly low temperature to hinder the exothermic reaction of magnesium and simultaneously provide conditions for the metal completely filled the cavity, avoiding misruns or cold lap.

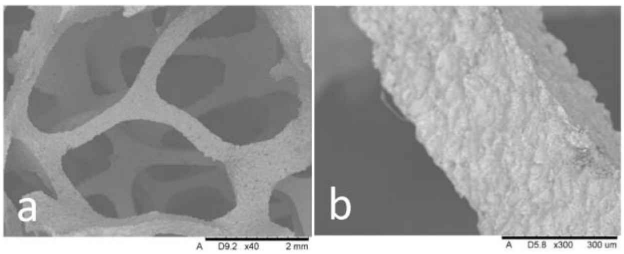

Fig. 3. Structure of AZ91 10 PPI foam (a), single strut with surface affected by casting process and interaction with moulding material (b)

Liquid magnesium exposed to the atmosphere oxidizes very willingly releasing heat that automatically accelerate reaction. Therefore, a protective gas mixture of SF_6/CO_2 should be applied. Unfortunately, during pouring in the autoclave, some amount of air penetrates through the walls of the mould. Locally, oxidation may increase the temperature over 1200°C and then a component of moulding $CaSO_4$ decomposes to CaO, SO_2 and oxygen, which intensifies the reaction leading to gas pressure increase and even explosion. Hence, controlling the temperature parameters during the pouring and cooling of the casting is very important. Moreover, at moderate interaction of the liquid magnesium with the mould mass, which includes silicon oxide, Mg_2Si may form according to the formula (2):

$$4Mg + SiO_2 \rightarrow 2MgO + Mg_2Si \tag{2}$$

These crystals are usually segregated along the casting's surface (see Fig. 4a), growing deeper if the temperature is too high. Therefore, the process was developed and parameters were precisely controlled. Such inclusions induced intergranular corrosion and degradation in an entire relatively small volume of the foam. Additionally, Vyas et al. [23] indicated that $MgAl_2O_4$ and Mg_2SiO_4 cab be formed at the surface of AZ91, when metal reacts with mould components like alumina or silica binder. Elaborated process parameters, especially temperature of the mould and poured metal, as well as effective protection gas system, allow the formation of a continuous MgS layer and manufacturing standard AZ91 microstructure (Fig. 4b).

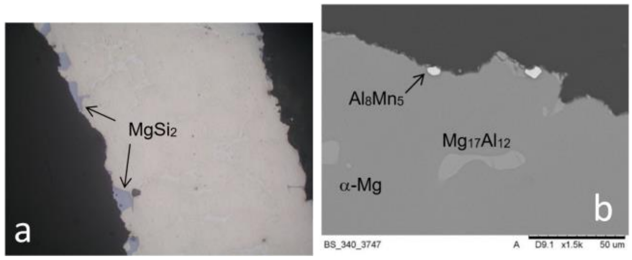

Fig. 4. Formation of Mg_2Si at the surface due to interaction with moulding material at higher process temperature (620°C mould / 740°C metal) (a), microstructure with typical for AZ91intermetallic phases (b)

On the surface of the foam structure, some components originated from moulding material (Fig.5) were observed, which were further washed out with a water solution of acetic acid.

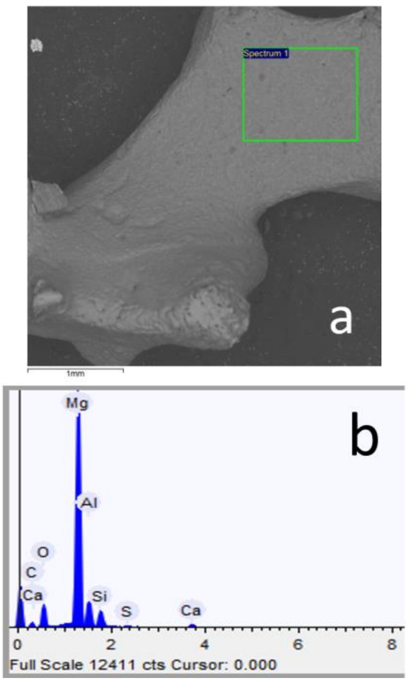

Fig. 5. Chemical analysis of the strut surface confirming elements originated from the moulding materials

In order to reduce the reaction of the metal with the mould, the temperature and contact time should be as low as possible. Under these conditions, the metal should flow in and fill the network of tiny joints in the mould cavity. Experimental determination of the temperature after pouring close to the cavity shows that it drops very slowly (dT/dt≈4.5°C/min for the first minutes). Thus, to limit the chemical interaction, contact time of liquid metal with ceramic mould must be possibly short. The metal should flow only through the necessary length of the channels and solidify immediately. For this purpose, minimum mould and metal temperatures should be selected. Flow penetration distance of poured metal in a cylindrical channel of d diameter can be estimated from Flemings formula [24-26]. It presumes that flow at constant velocity V_1 stops when half of the metal volume solidifies and chokes the channel. The following mathematical model of L distance is as follows in formula (3):

$$L = \frac{\rho_1\, d\, V_1}{2h_{12}(T_m - T_2)}\left(\Delta H + C_{p1}(T_p - T_m)\left(1 + \frac{h_{12}}{2K_2}\sqrt{\frac{\pi\alpha_2 x_2}{V_1}}\right)\right) \qquad (3)$$

where used parameters are described in Table 1. The calculated values of the distance for selected temperature values are presented in Fig. 6.

Table 1.
The investment casting parameters and thermo-physical properties of the mould and AZ91 alloy.

Parameter	Description	Unit	Value
V_1 (10 PPI)	metal flow velocity	cm/s	5.856
V_1 (20 PPI)	metal flow velocity	cm/s	3.294
α_2	thermal diffusivity of mould	cm^2/s	0.00747
p_1	density	g/cm^3	1.810
ΔH	heat of fusion	J/g	373
c_{p1}	specific heat capacity	J/(g·°C)	1.047
T_p	pouring temperature	°C	720
T_m	melting temperature	°C	595
h_{12}	heat transfer coefficient between AZ91-mould	W/cm^2·°C	0.060
K_2	thermal conductivity	W/(cm·C)	0.005
T_2	mould temperature	°C	550
x_2	strut/choking length	cm	0.120
d (10 PPI)	strut thickness	cm	0.020
d (20 PPI)	strut thickness	cm	0.015

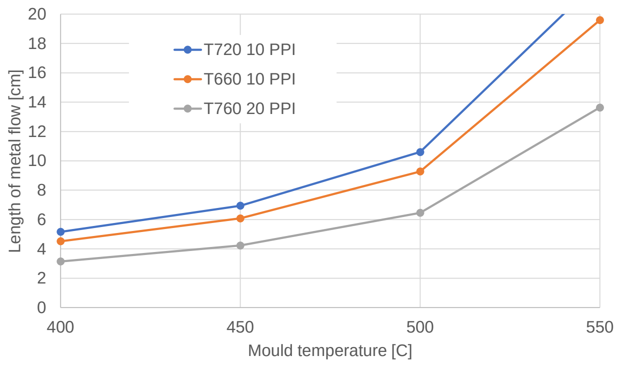

Fig. 6. Calculated length of metal flow (penetration distance) in preheated mould (400-550°C) for pouring temperature 660-760°C in cavity produced from 10 or 20 PPI polyurethane foam.

Foam characterised by the parameter of 10 PPI has larger cross-sections of the channels (strut), therefore the distance to penetrate is greater. The total size of the foams was usually 4x4x6 cm, so assuming that the consecutive struts made an equal connection, the minimum track length is 6 cm. For such a geometry and 10 PPI foam, it can be read from the diagram that the mould temperature should be 450°C if the metal is poured at 660°C. Much more difficult conditions for filling are for foam with a greater number of pores (20 PPI), but therefore with a smaller thickness of the struts. The mould should be heated to 500°C, and the metal to 760°C. Experimental observations have shown that such temperatures are too high. Too much of the Mg_2Si precipitate led to the blackening of the surface of the casting, however it occurred also on foams that were kept in hot mould for too long. Rapid cooling of moulds and foams in water after approx. 2 minutes has proved to reduce the samples' surface blackening and burning. It can be concluded that casting magnesium alloys in ceramic masses requires very precise selection of the process parameters. Especially in the case of thin-walled structures and high surface exposure. In subsequent stages of the research, 3D prints were used as patterns. In their case, it is much easier to control the process, obtaining a very good surface quality. Temperatures up to 720°C can be used since it is the upper limit for AZ91 casting, above which oxidation and combustion danger increase [27].

3.2 Compressive behaviour

Quasi-static compression tests have shown that the magnesium foams behave with typical for metallic foams mechanism – initially deforming elastically, then compressing without stress raise, and finally when the foam densifies – raising the stress rate dramatically, as shown in Fig. 7.

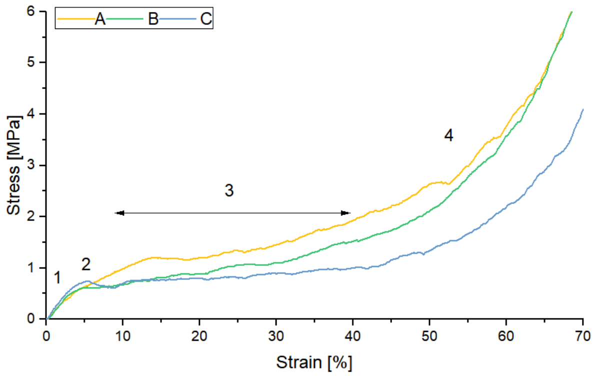

Fig. 7. Stress-strain curves of AZ91 foam samples, performing with typical for metallic foams regions: 1 – elastic strain, 2 – plastic bulking, 3 – plateau phase, 4 – densification

The foams have performed depending on their porosity and average pore size. Typically, the foams of lower porosities and of smaller pore size performed with higher Young's modulus and better energy absorption values. Their compressive strength also depended greatly on the struts' thickness (depending on the thickness of wax slurry layer on PUR pattern). The foam C presented in Fig. 7 had an average pore size 20 PPI and porosity equal 87.5% performing with Young's modulus equal to 25.4 MPa and with specific energy absorption 2.8 J/g. Other researched foams of similar parameters have shown SEA up to 9,5 J/g, which is in similar value range as open-cell aluminum foams produced by space holder method by Hajizadeh et al. in [28]. The SEA value was calculated according to formula (4), where sf is compression distance, and mf is linear density:

$$SEA = \frac{\int_0^{s_f} F\,ds}{m_f * s_f} \tag{4}$$

The crushed foams were observed under SEM microscope to determine their collapsing mechanism. Figure 8 shows a piece of crushed foam with struts either bent or broken, proving that the AZ91 foam shows plastic-brittle collapsing mechanism. Majority of the foams struts were broken or cracked (blue arrows), but some were necked, bent or twisted (yellow arrows). That happens because the foams struts in the deforming process are not only compressed, but also stretched, bent and twisted in all directions due to their connections with variously angled struts and strut joints.

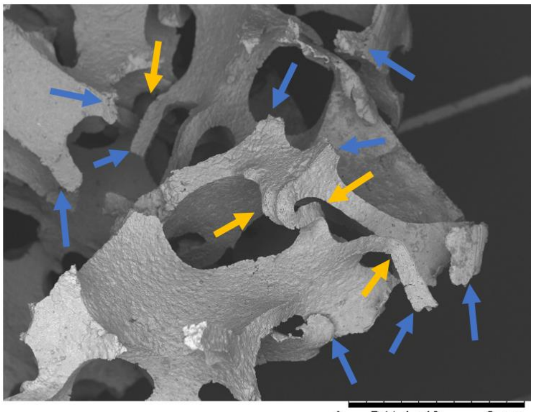

Fig. 8. SEM image of crushed AZ91 foam sample with visible brittle (blue arrows) and plastic (yellow arrows) deformations

4. Conclusions

A method of investment magnesium foam casting was developed. The most important parameters of the process, its limitations and effect on the foam structure were discussed. Characteristics of the foam microstructure, reaction with the moulding mass and inclusions on its surface are presented. It can be concluded that:

- The casting parameters have to be matched with foams size and porosity to obtain a clean surface and full mould filling;
- The foams during casting process react with gypsum-based moulding masses at high temperatures and prolonged cooling times, resulting in Mg_2Si inclusions on the metal surface;
- The foams of average 20 PPI pore size and >80% porosity perform with Young's modulus values of average 30 MPa;
- The AZ91 foams during collapsing deform both plastically and in a brittle way, with a majority of brittle deformations;
- Specific energy absorption of obtained magnesium foams is comparable with aluminum foams of higher density.

Conflict of interests

The authors declare that they have no conflicts of interests

References

[1] Gawdzińska, K., Chybowski, L. & Przetakiewicz, W. (2017). Study of thermal properties of cast metal- ceramic composite foams. *Archives of Foundry Engineering*. 17(4), 47-50. DOI:10.1515/afe-2017-0129.

[2] Bisht, A., Patel, V. K. & Gangil, B. (2019). Future of metal foam materials in automotive industry. In: Katiyar, J., Bhattacharya, S., Patel, V., Kumar, V. (eds), *Automotive Tribology. Energy, Environment, and Sustainability* (pp. 51-63). Singapore: Springer. DOI:10.1007/978-981-15-0434-1_4.

[3] Popielarski, P., Sika, R., Czarnecka-Komorowska, D., Szymański, P., Rogalewicz, M. & Gawdzińska, K. (2021). Evaluation of the cause and consequences of defects in cast metal-ceramic composite foams. *Archives of Foundry Engineering*. 21(1), 81-88. DOI:10.24425/afe.2021.136082.

[4] Vilniškis, T., Januševičius, T. & Baltrėnas, P. (2020). Case study: Evaluation of noise reduction in frequencies and sound reduction index of construction with variable noise isolation. *Noise Control Engineering Journal*. 68(3), 199-208. DOI:10.3397/1/376817.

[5] Sivasankaran, S. & Mallawi, F.O.M. (2021). Numerical study on convective flow boiling of nanoliquid inside a pipe filling with aluminum metal foam by two-phase model. *Case Studies in Thermal Engineering*. 26, 101095, 1-14. DOI:10.1016/J.CSITE.2021.101095.

[6] Naplocha, K., Koniuszewska, A., Lichota, J. & Kaczmar, J. W. (2016). Enhancement of heat transfer in PCM by cellular Zn-Al structure. *Archives of Foundry Engineering*. 16(4), 91-94. DOI:10.1515/afe-2016-0090.

[7] Lehmann, H., Werzner, E., Malik, A., Abendroth, M., Ray, S. & Jung, B. (2022). Computer-aided design of metal melt filters: geometric modifications of open-cell foams, effective hydraulic properties and filtration performance. *Advanced Engineering Materials*. 24(2), 1-11. DOI:10.1002/adem.202100878.

[8] Kryca, J., Iwaniszyn, M., Piątek, M., Jodłowski, P.J., Jędrzejczyk, R., Pędrys, R., Wróbel, A., Łojewska, J. & Kołodziej, A. (2016). Structured foam reactor with CuSSZ-13 catalyst for SCR of NOx with ammonia. *Topics in Catalysis.* 59(10), 887-894. DOI:10.1007/S11244-016-0564-4.

[9] Alamdari, A. (2015). Performance assessment of packed bed reactor and catalytic membrane reactor for steam reforming of methane through metal foam catalyst support. *Journal of Natural Gas Science and Engineering*. 27(2), 934-944. DOI:10.1016/J.JNGSE.2015.09.037.

[10] Anglani, A. & Pacella, M. (2021). Binary Gaussian Process classification of quality in the production of aluminum alloys foams with regular open cells. *Procedia CIRP*. 99, 307-312. DOI:10.1016/j.procir.2021.03.046.

[11] Anglani, A. & Pacella, M. (2018). Logistic regression and response surface design for statistical modeling of investment casting process in metal foam production. *Procedia CIRP*. 67, 504-509. DOI:10.1016/J.PROCIR.2017.12.252.

[12] Wang, Y., Jiang, S., Wu, Z., Shao, H., Wang, K., & Wang, L. (2018). Study on the inhibition influence on gas explosions by metal foam based on its density and coal dust. *Journal of Loss Prevention in the Process Industries*. 56, 451-457. DOI:10.1016/J.JLP.2018.09.009.

[13] Hua, L., Sun, H. & Gu Jiangsu, J. (2016). Foam metal metamaterial panel for mechanical waves isolation. Proceedings of the SPIE, 9802 (id.98021R), 8. DOI:10.1117/12.2219470.

[14] Marx, J., & Rabiei, A. (2017). Overview of composite metal foams and their properties and performance. Advanced Engineering Materials, 19(11), 1600776. DOI:10.1002/ADEM.201600776.

[15] Wong, P., Song, S., Tsai, P., Maqnun, M.J., Wang, W., Wu, J. & Jang, S.J. (2022). Using Cu as a spacer to fabricate and control the porosity of titanium zirconium based bulk metallic glass foams for orthopedic implant applications. *Materials*. 15(5), 1887, 1-14. https://doi.org/10.3390/ma15051887.

[16] Kang, L., Shi, Y. & Luo, X. (2021). Effects of sodium chloride on structure and compressive properties of foamed AZ91 Effects of sodium chloride on structure and compressive properties of foamed AZ91. *AIP Advances.*11, 015118, 1-4. DOI:10.1063/5.0033314.

[17] Pelczar, D., Długosz, P., Darłak, P., Nykiel, M., & Hebda, M. (2022). The effect of BN or SiC addition on PEO properties of coatings formed on AZ91 magnesium alloy. *Archives of Metallurgy and Materials.* 67(1), 147-154. DOI: https://doi.org/10.24425/amm.2022.137483.

[18] Gupta, M., Mui Ling Sharon, N. (2010). *Magnesium, Magnesium Alloys, and Magnesium Composites*. Hoboken: John Wiley & Sons, Ltd. DOI:10.1002/9780470905098.

[19] Dong-hui, Y., Shang-run, Y., Hui, W., Ai-bin, M., Jing-hua, J., Jian-qing, C. & Ding-lie, W. (2010). Compressive properties of cellular Mg foams fabricated by melt-foaming method. *Materials Science & Engineering A*. 527(21-22), 5405-5409. DOI:10.1016/j.msea.2010.05.017.

[20] Kroupová, I., Radkovský, F., Lichý, P. & Bednářová, V. (2015). Manufacturing of cast metal foams with irregular cell structure. *Archives of Foundry Engineering*. 15(2), 55-58. DOI:10.1515/afe-2015-0038.

[21] Shih, T., Wang, J. & Chong, K. (2004). Combustion of magnesium alloys in air. Materials Chemistry and Physics. 85(2-3), 302-309. DOI:10.1016/j.matchemphys.2004.01.036.

[22] Fujisawa, S., Yonezu, A. (2014). Mechanical property of microstructure in die-cast magnesium alloy evaluated by indentation testing at elevated temperature. *Recent Advances in Structural Integrity Analysis: Proceedings of the International Congress (APCF/SIF-2014).* Woodhead Publishing Limited. 422-426. DOI:10.1533/9780081002254.422.

[23] Vyas, A.V. & Sutaria, M.P. (2020). Investigation on influence of the cast part thickness on interfacial mold–metal reactions during the investment casting of AZ91 magnesium alloy. I*nternational Journal of Metalcasting*. 20(4), 139-144. DOI:10.1007/s40962-020-00530-2.

[24] Ravi, K.R., Pillai, R.M., Amaranathan, K.R., Pai, B.C. & Chakraborty, M. (2008). Fluidity of aluminum alloys and composites: A review. *Journal of Alloys and Compounds*. 456(1-2), 201-210. DOI:10.1016/j.jallcom.2007.02.038.

[25] Voigt, R.C., Bertoletti, J., Kaley, A., Ricotta, S., Sunday, T. (2002). *Fillability of thin-wall steel castings*. Technical Report. https://doi.org/10.2172/801749.

[26] Dewhirst, B.A. (2008). *Castability control in metal casting via fluidity measures: Application of error analysis to Variations in Fluidity Testing*. Worcester Polytechnic Institute.

[27] Le, Q., Zhang, Z., Cui, J. & Chang, S. (2009). Study on the filtering purification of AZ91 magnesium alloy. *Materials Science Forum*. 610-613, 754-757. DOI:10.4028/www.scientific.net/MSF.610-613.754.

[28] Wong, P., Song, S., Tsai, P., Maqnun, M.J., Wang, W., Wu, J. & Jang, S.J. (2022). Using Cu as a spacer to fabricate and control the porosity of titanium zirconium based bulk metallic glass foams for orthopedic implant applications. Materials. 15(5), 1887, 1-14. https://doi.org/10.3390/ma15051887.